An Implantable 64-channel Neural Interface with Reconfigurable Recording and Stimulation

Jesse J. Wheeler, Keith Baldwin, Alex Kindle, Daniel Guyon, Brian Nugent, Carlos Segura, John Rodriguez, Andrew Czarnecki, Hailey J. Dispirito, John Lachapelle, Philip D. Parks, James Moran

Charles Stark Draper Laboratory, Cambridge, MA
jwheeler@draper.com

Alik S. Widge[a,b], Darin D. Dougherty[a], Emad N. Eskandar[c]

[(a)] Department of Psychiatry, Massachusetts General Hospital and Harvard Medical School, Boston, MA
[(b)] Picower Institute for Learning & Memory, Massachusetts Institute of Technology, Cambridge, MA
[(c)] Department of Neurological Surgery, Massachusetts General Hospital, Harvard Medical School, Boston, MA

Abstract - Next generation implantable medical devices will have the potential to provide more precise and effective therapies through adaptive closed-loop controllers that combine sensing and stimulation across larger numbers of electrode channels. A major challenge in the design of such devices is balancing increased functionality and channel counts with the miniaturization required for implantation within small anatomical spaces. Customized therapies will require adaptive systems capable of tuning which channels are sensed and stimulated to overcome variability in patient-specific needs, surgical placement of electrodes, and chronic physiological responses. In order to address these challenges, we have designed a miniaturized implantable fully-reconfigurable front-end system that is integrated into the distal end of an 8-wire lead, enabling up to 64 electrodes to be dynamically configured for sensing and stimulation. Full reconfigurability is enabled by two custom 32x2 cross-point switch (CPS) matrix ASICs which can route any electrode to either an amplifier with reprogrammable bandwidth and integrated ADC or to one of two independent stimulation channels that can be driven through the lead. The 8-wire circuit includes a digital interface for robust communication as well as a charge-balanced powering scheme for enhanced safety. The system is encased in a hermetic package designed to fit within a 14 mm bur-hole in the skull for neuromodulation of the brain, but could easily be adapted to enhance therapies across a broad spectrum of applications.

Keywords – Neural stimulation - Deep brain; Neural interfaces - Implantable systems; Neural interfaces - Microsystems and microfabrication

I. INTRODUCTION

A. Challenges for Advanced Neural Interfaces

Advanced neural interface technology has the potential to provide enhanced therapies through coordinated multi-site responsive neuromodulation. The combination of high density electrodes, multi-modal recordings, and adaptive closed-loop stimulation will enable precision micro-therapies to be applied at exactly the right time and location with minimal side-effects to patients. Past approaches using open-loop implantable pulse generators attached to passive leads through large headers and lead connectors have not scaled well to higher channel counts and have lacked essential functionality like embedded closed-loop processing. More recent systems have achieved either higher channel-counts or closed-loop stimulation, but not both simultaneously [1-4]. In addition to these challenges, clinical translation of implantable devices requires careful design and testing to demonstrate chronic safety, reliability, and effectiveness. Key safety considerations include low thermal dissipation, electrostatic discharge survivability, electromagnetic interference, single-fault tolerance, and DC-leakage into the body.

B. Distributed Satellite-Hub System Architecture

To overcome many of these challenges previously described, we have designed an implantable closed-loop neuromodulation system based upon a distributed modular satellite-hub architecture, shown in Figure 1. This architecture consists of 1) multiple implantable satellite micro-electronics modules, each providing interfaces to high-density electrodes through standard 8-wire leads, 2) an implantable centralized hub electronics module, that provides power, processing, telemetry, and system control, and 3) an external base station, that is used to recharge and reprogram the implanted device, as well as stream neural data to a computer for analysis, visualization, and clinical

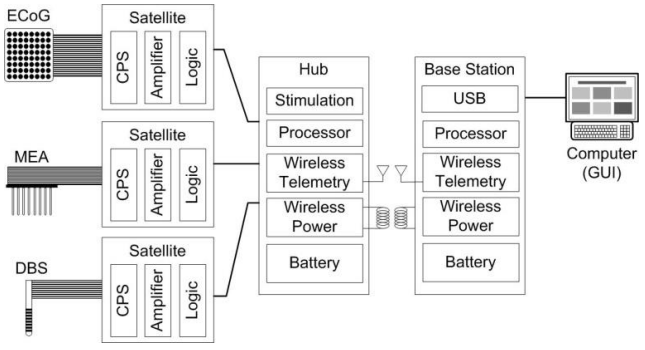

FIGURE 1: SYSTEM-LEVEL BLOCK DIAGRAM HIGHLIGHTING MAJOR FUNCTIONAL COMPONENTS WITHIN OUR DISTRIBUTED ARCHITECTURE. THE SCALABLE SYSTEM INCLUDES SATELLITES THAT CAN INTERFACE WITH A WIDE VARIETY OF HIGH-DENSITY ELECTRODES AND A HUB THAT CAN CONNECT TO FIVE SATELLITES FOR A TOTAL OF 320 MULTI-MODAL ELECTRODES

control. Satellite modules include a cross-point switch module, which allows 64 electrodes to be configured in real-time for recording or stimulation, and a neural amplifier with embedded ADC that enables robust digital transmission of neural data to the hub through a reduced channel count. The hub includes 8 independent stimulation channels, a low-power FPGA and ARM processor for adaptive closed-loop control, bi-directional wireless data telemetry to the external base station, and a wirelessly re-chargeable lithium battery for extended operation. A standard 8-channel connectorized lead interface is used to connect between the satellites and hub, which includes two independent analog stimulus channels, AC power, and bi-directional charged-balanced digital communication.

Advantages of this modular distributed architecture over single-package monolithic designs include improved noise immunity by amplifcation and digitization near the signal sources, overall volume reduction in critical anatomical regions where electrodes are implanted, and improved scalability toward higher electrode channel counts that may be dispersed across multiple distant locations. While the initial application is focused on adaptive cortical and subcortical neuromodulation, the flexible architecture is amenable to applications targeting numerous other diseases, including but not limited to closed-loop motor, cardiac, pulmonary, pain, bladder, and hormonal control. The following focuses on the design and performance of the satellite module.

II. Satellite Module Design

A. Cross-Point Switch Matrix

Two 32x2 custom neural cross-point switch (CPS) ASICs provide clinicians and researchers the ability to configure any electrode for recording, stimulation, or open-circuit, as shown in Figure 2. Each CPS ASIC supports recording from up to 32 electrodes (64 total), or can be dynamically reconfigured for stimulation, where any electrode can be tied to either of the two analog stimulus lines. A variety of stimulation montages are possible, including routing of a single stimulus line to multiple electrodes simultaneously to create larger-area stimulation sites comprised of multiple electrode contacts. The CPS ASIC is fabricated using a high-voltage 180nm CMOS process enabling transmission of +/- 9V stimulation signal ranges in the current version, which will be increased to +/- 20V in the next version. Each ASIC consumes less than 500 uW on average, is configured via a 4-wire 1.8V SPI interface, and contains protection circuitry to guard from ESD and ESU/Defib events.

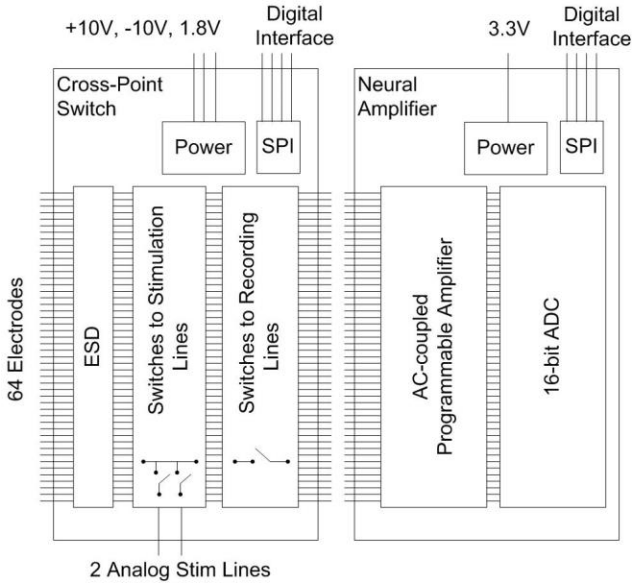

FIGURE 2: BLOCK DIAGRAM OF THE FRONT-END INTERFACE THAT ENABLES ON-DEMAND RECONFIGURATION OF 64 ELECTRODES FOR RECORDING AND STIMULATION

B. Neural Amplifier

A re-configurable low-noise neural amplifier ASIC (Intan RHD2164) provides flexibility in tuning bandwidth and sampling rate for full-bandwidth (0.1Hz-7.5kHz), single-unit (500Hz-7.5kHz), and local field potential (LFP) or electrocorticographic (ECoG) (0.1Hz-200Hz) recordings, as shown in Figure 2. The Intan ASIC combines 64 amplifiers, analog and digital filters, a multiplexed 16-bit analog-to-digital converter (ADC), and auxiliary measurements of internal satellite temperature, supply voltage rails (3.3V, 1.8V, and 1.2V), and multi-frequency electrode impedances. Additionally, individual amplifier channels can be shut-down to optimize power when not needed. The ASIC also includes "fast-settle" functionality for rapid recovery from stimulation artifacts.

C. AC Power Management

Power transfer to the satellite from the hub must not result in significant DC leakage, which can lead to long-term bodily harm. Typical medical-grade connectors do not achieve isolation above 200 kΩ, which could result in as much as 50µA of sustained DC current from a 10V supply.

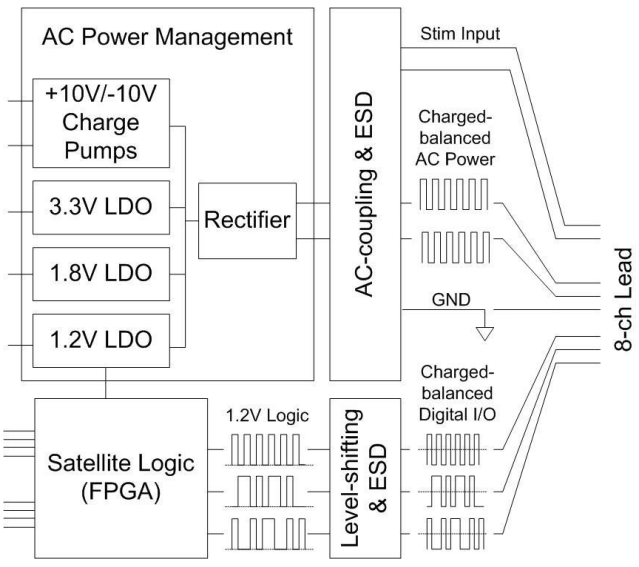

FIGURE 3: BLOCK DIAGRAM OF THE AC POWER MANAGEMENT ASIC AND SATELLITE LOGIC, HIGHLIGHTING THE CHARGED-BALANCED INTERFACE OVER AN 8-CH LEAD

To mitigate the challenges of DC-leakage, a charge-balanced AC power scheme is employed using two complimentary 3.7V 1MHz square-wave signals supplied by the hub module. A custom power management ASIC fabricated using a high-voltage 180nm CMOS process is used to convert the AC power signals to DC and then regulate 3.3V, 1.8V, and 1.2V supplies for the amplifier, CPS, and satellite logic, respectively. Additional on-board Pelliconi charge-pumps are used to generate the +/-9V supplies required to pass full-range stimulation signals through the CPS, as shown in Figure 3.

D. Satellite Logic with Charge-balanced Communication

Satellite logic is implemented with a low power Microsemi IGLOO Nano FPGA, which controls the CPS and amplifier ASICs, and monitors vital system health sensors for safety. The logic also performs data compression, packetization, error-checking, and DC-balanced coding for communication with the hub. Charged-balanced communication with the hub is achieved by both the DC-balanced digital code that ensures equal density of 1's and 0's in data packets, and level-shifting circuitry that translates between the 1.2V voltage logic used by the FPGA and balanced +/- 0.6V digital I/O signals transmitted across the satellite-hub lead. Communication between the satellite and hub is achieved through three digital I/O lines (CLK, MOSI, and MISO) with clock speeds ranging from 3-25MHz, depending upon the recording configuration. All interfacial lines are protected by blocking capacitors and ESD circuits designed to meet FDA standards for human use, as shown in Figure 3.

E. Assembly and Packaging

In its final form, electronics for the front-end satellite will be assembled on a 4-layer hybrid rigid-flex board containing bare silicon, chip scale packages, and passives. The rigid-flex board will fold into a compact volume and attached directly to Pt/Ir feedthrough pins that are bonded directly to electrodes (single-unit, ECoG, or DBS) and lead wires outside a hermetically-sealed Ti enclosure. External bonds to the feedthrough pins will be overmolded in epoxy for improved mechanical strength and electrical isolation between bonds, and fitted with a flexible rubber cap with embedded anchors for affixing to the skull within a standard 14 mm diameter burr hole, as shown in Figure 4.

FIGURE 4: FINAL SATELLITE ASSEMBLY FITS IN A 14-MM DIAM HERMETIC ENCLOSURE DESIGNED TO SIT WITHIN A STANDARD CRANIAL BURR-HOLE. THE SATELLITE CAN BE ATTACHED TO ANY VARIETY OF ELECTRODE TYPES.

III. SATELLITE MODULE PERFORMANCE

A. Satellite Prototype and Benchtop Tests

In order to demonstrate functionality and evaluate system performance, a prototype satellite electronics module was fabricated on a rigid PCB with stimulation waveforms generated by an external programmable stimulator ASIC (Cactus Semiconductor CSI021). Individual component testing as well as overall system performance was evaluated on benchtop using a phantom brain to mimic the expected *in vivo* environment prior to subsequent animal studies. The phantom brain model was constructed from conductive gelatin with neural signals simulated from an embedded dipole driven by the audio output of a laptop computer. Neural signals played through the phantom brain were derived from actual single-unit recordings from a behaving monkey. Key results from benchtop tests are provided in the following sections.

B. CPS Electrical Characteristics

Impedances of the recording and stimulation switches IN the CPS ASIC in both "on" and "off" configurations were measured with an Autolab PGSTAT12 (Eco Chemie, Utrecht, Netherlands) with built-in frequency response analyzer (FRA2, Brinkmann Instruments, Westbury, NY) in response to voltage-controlled 25 mV (rms) sinusoids. As shown in Figure 5, "on" impedances for both stimulation and recording were uniformly flat up to 100kHz at approximately 75 Ohms. This low impedance is desirable for both recording and stimulation and is only a fraction of the impedance of both micro- and macro-scale electrodes. "Off" impedances were greater than 10MΩ for frequencies less than 10kHz and above 100kΩ up to 100kHz, which ensures high channel-to-channel isolation.

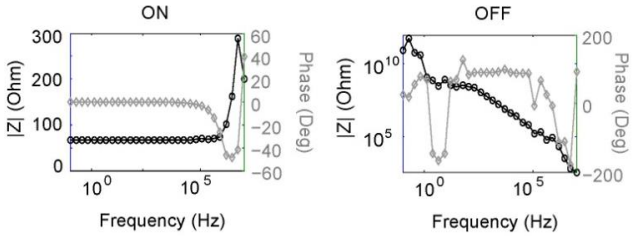

FIGURE 5: IMPEDANCE CHARACTERISTICS OF THE CPS SHOWING LOW IMPEDANCES AND PHASE DISTORTION IN THE "ON" STATE AND HIGH ISOLATION IN THE "OFF" STATE

C. Rapid Switching for Multi-channel Stimulation

Rapid reconfiguration of multiple electrodes for stimulation was evaluated by cycling pulses from a single stimulation line to several electrodes at high speed. The bi-phasic pulse train was generated by an external Cactus ASIC, which would be located in the central hub in our final system. Individual pulses were sequentially routed through the CPS in the satellite module to individual electrodes on a cortical electrode paddle array (2 mm Pt contacts) placed on the brain phantom. As shown in Figure 6, charge-

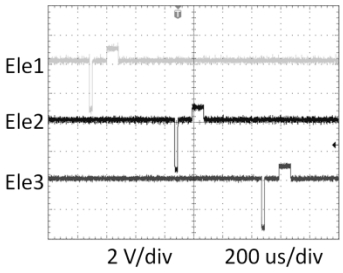

FIGURE 6: RAPID SWITCHING OF SINGLE STIMULUS CHANNEL THROUGH ELECTRODES

balanced pulses from a single stimulation input channel could be rapidly routed to individual electrodes without distortion or cross-talk on adjacent disconnected electrodes. With a 10 MHz SPI clock speed, the CPS could be reconfigured in less than 6.5 µs, which allows high-channel count stimulation with reduced numbers of stimulus drivers.

D. Amplifier Noise

The input-referred noise of the amplifier was measured by shorting amplifier inputs (including reference) to ground. The mean+/-sem for full-bandwidth recordings (0.1Hz-10kHz) was 2.87+/-0.63 µVrms and for spike-only recordings (500Hz-7.5kHz) was 2.45+/-.58 µVrms. These noise levels are sufficient for high-resolution action potential recordings, which typically range in magnitude from 100's µVp-p to several mV's p-p. Noise levels for LFP and ECoG recordings were also evaluated. Noise in the alpha-band (7.5Hz-12.5Hz) and beta-band (15Hz-30Hz), where the depth of modulated power is in the range of 10s of µVrms, was 346+/-86 ηVrms and 397+/-105 ηVrms, respectively. Noise in the gamma-band (75Hz-115Hz), where the depth of modulated power is in the range of 1-2 µVrms, was 314+/-69 ηVrms.

E. Recording and Stimulation

The combination of recording and stimulation was evaluated by recording simulated neural signals derived from the brain phantom and periodically switching electrodes between recording and stimulation modes. Figure 7 shows neural recording and stimulation with the amplifier configured for spike recordings (500Hz-7.5kHz). As shown, simulated neural signals could be reliably detected on the recording channel (an example recorded action potential is highlighted). At approximately 0.9s, the channel was switched to stimulation mode, which disconnected the amplifier while pulse trains were delivered to the phantom brain. About a second later, the channel was switched back to recording mode, which re-connected the amplifier. Transient artifacts from switching were less than a couple ms for spike-recordings, but became more persistent when amplifier bandwidths were increased for low-frequency recordings. Work toward the optimization of stimulus artifact suppression is ongoing. This satellite architecture offers a variety of methods to artifact suppression, enabling a multi-layered approach using coordinated switching, amplifier fast-settling, and embedded signal processing.

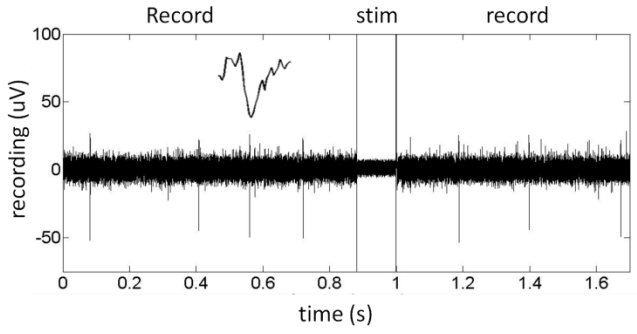

FIGURE 7: RAPID RECONFIGURATION OF AN ELECTRODE FOR RECORDING AND STIMULATION. ACTION POTENTIALS ARE CLEARLY VISIBLE WITH ONE ACTION POTENTIAL HIGHLIGHTED DIRECTLY ABOVE ITS OCCURANCE IN THE RECORDING. HIGH ISOLATION OF THE CPS IS SHOWN BY THE LACK OF CROSS-TALK INTO THE AMPLIFIER RECORDING WHILE A STIMULATION PULSE TRAIN WAS APPLIED

IV. CONCLUSION

The scalable satellite-hub architecture presented here enables the use of higher channel-counts of multi-modal electrodes in addition to more precise and coordinated responsive neuromodulation. This enhancement of functionality is achieved with simultaneous miniaturization for implantation in small anatomical spaces. Satellite electronics modules were shown to achieve high-fidelity neural recordings with the fully-reconfigurable amplifier, which will provide access to richer neural data sets that include single-units, LFPs, and ECoG. Multi-modal data will allow researchers and clinicians to better diagnose diseases, develop more powerful decoders and controllers, and explore network behavior of neural systems. On-demand reconfigurability of high-density electrodes will provide greater customization of neuromodulation therapies, where the system can adapt to chronic changes caused by neural plasticity, reactive tissue responses, and evolving patient needs.

While satellite modules presented here will be packaged specifically for implantation within the skull and attached to cortical and subcortical electrodes, modules could be easily adapted for implantation in other areas of the body and attached to a variety of electrodes. For example, satellite modules could be used for both neural and muscular interfaces in the periphery or viscera as part of a therapeutic device targeting sensorimotor, hypertension, cardiovascular, diabetes, or pain disorders. Key functional blocks (e.g, CPS) could also be used to augment existing devices, allowing clinicians and researchers greater flexibility with preferred amplifier or stimulation systems.

ACKNOWLEDGEMENT

This work was supported by the Defense Advanced Research Projects Agency (DARPA), Biological Technologies Office (BTO), under contract number W911NF-14-2-0045. The opinions presented are those of the authors alone and not of DARPA, Charles Stark Draper Laboratory, or Massachusetts General Hospital.

REFERENCES

[1] D. A. Borton, *et al.*, "An implantable wireless neural interface for recording cortical circuit dynamics in moving primates," *J Neural Eng,* vol. 10, p. 026010, Apr 2013.

[2] F. T. Sun and M. J. Morrell, "The RNS System: responsive cortical stimulation for the treatment of refractory partial epilepsy," *Expert Rev Med Devices,* vol. 11, pp. 563-72, Nov 2014.

[3] P. H. Peckham, *et al.*, "An advanced neuroprosthesis for restoration of hand and upper arm control using an implantable controller," *J Hand Surg Am,* vol. 27, pp. 265-76, Mar 2002.

[4] S. Stanslaski, *et al.*, "Design and validation of a fully implantable, chronic, closed-loop neuromodulation device with concurrent sensing and stimulation," *IEEE Trans Neural Syst Rehabil Eng,* vol. 20, pp. 410-21, Jul 2012.